RESEARCH PAPER

Anti-melanogenesis potential effect of green alginate nanoparticle of kojic acid as skin whitening product: *in-vitro* and *in-vivo* evaluation

Mahmoud Omidi[1,2], Majid Saeedi[3], Hannaneh Shahlavi[4], Seyyed Mobin Rahimnia[3], Saeed Azimi[1,5], Esmaeil Mohammadian[6,7*], Seyyed Mohammad Hassan Hashemi[1,8*]

[1] *Food Health Research Center, Hormozgan University of Medical Sciences, Bandar Abbas, Iran*
[2] *Department of Pharmacology and Toxicology, Faculty of Pharmacy, Hormozgan University of Medical Sciences, Bandar Abbas, Iran*
[3] *Department of Pharmaceutics, Faculty of Pharmacy, Mazandaran University of Medical Sciences, Sari, Iran*
[4] *Student Research Committee, Faculty of Pharmacy, Hormozgan University of Medical Sciences, Bandar Abbas, Iran*
[5] *Department of Clinical Pharmacy, Faculty of Pharmacy, Hormozgan University of Medical Sciences, Bandar Abbas, Iran*
[6] *Cellular and Molecular Research Center, Research Institute for Health Development, Kurdistan University of Medical Sciences, Sanandaj, Iran*
[7] *Department of Medicinal Chemistry, School of Pharmacy, Hormozgan University of Medical Sciences, Bandar Abbas, Iran*
[8] *Department of Pharmaceutics, Faculty of Pharmacy, Hormozgan University of Medical Sciences, Bandar Abbas, Iran*

ABSTRACT

Objective(s): This study evaluated a novel method combining ionic gelation and ultrasound for producing kojic acid (KJA)-loaded sodium alginate (AL) nanoparticles to enhance dermal delivery and anti-pigmentation effects.

Material and methods: Green and eco-friendly preparation of nanoparticles, inspection of nanoparticle features, checking structure, animal safety administration, cellular vitality, and inhibitory evaluation of melanin synthesis were employed.

Results: The results showed that increasing the volume ratio of AL/$CaCl_2$ from 10:2 to 10:10 reduced the mean particle size from 1691.767 ± 118.095 nm to 338.533 ± 8.429 nm. Moreover, the encapsulation efficiency was enhanced with this increase, rising from 8.051 ± 3.035% to 78.770 ± 3.155%. Skin permeability tests indicated that the KJA-AL nanoparticle gel delivered more KJA to the dermal layers (39.470 ± 3.606% or 519.432 ± 47.465 µg/cm²) and the receptor compartment (15.210 ± 0.468% or 200.170 ± 6.161 µg/cm²) compared to the plain KJA gel. The optimum formulation exhibited fewer toxic effects on HFF (Human Foreskin Fibroblast) cells, while a significant cytotoxic effect was observed on B16F10 cells with the KJA-AL nanoparticle. The non-irritating effect of the KJA-AL nanoparticle gel was confirmed through a dermal irritation test on Wistar rats. Two additional advantages of the present study include: i) greater inhibition of melanin formation with KJA-AL nanoparticles compared to free KJA, and ii) significant inhibition of L-dopa auto-oxidation by KJA-AL nanoparticles (82.224 ± 2.079%) compared to KJA solution (55.829 ± 2.881%).

Conclusion: The results indicated that the KJA-AL nanoparticles produced in this study could serve as potential nano-vehicles for the dermal delivery of KJA. Additionally, they may offer an innovative solution for addressing hyper-melanogenesis-related issues.

Keywords: *Alginate, nanoparticle, Kojic acid, Anti-melanogenesis, Green preparation*

How to cite this article

Omidi M, Saeedi M, Shahlavi H, Rahimnia SM, Azimi S, Mohammadian E, Hashemi SMH. Anti-melanogenesis potential effect of green alginate nanoparticle of kojic acid as skin whitening product: in-vitro and in-vivo evaluation. Nanomed J. 2025; 12(4): 705-717. DOI: 10.22038/NMJ.2025.81428.2021

GRAPHICAL ABSTRACT

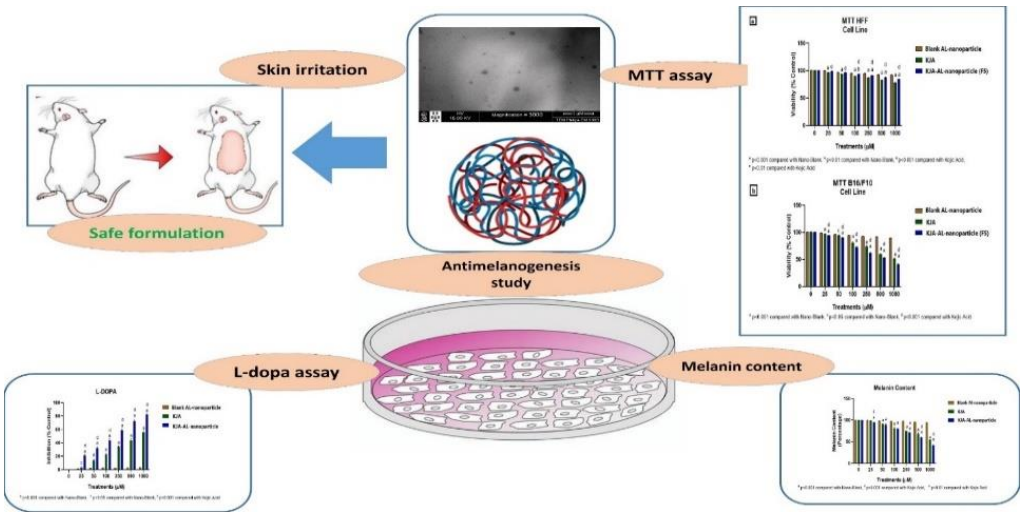

*Corresponding author(s) Emails: smhhashemipharma@gmail.com; e.mohamadyan1390@gmail.com.

Note. This manuscript was submitted on July 25, 2024; approved on September 28, 2024.

INTRODUCTION

Recent studies have highlighted the significance of therapeutic approaches for dermal issues, as dermal disorders are associated with increased levels of anxiety and depression in patients [1]. Dermal hyperpigmentation, particularly caused by sun exposure, commonly affects the sun-exposed areas of the face. Melasma is one of the most prevalent forms of persistent hyperpigmentation. Its global prevalence varies, ranging from 1% in the general population to 9-50% in high-risk populations. Additionally, this dermal condition can lead to psychological problems, including social isolation, depression, shame, anxiety, and a loss of social relationships [1]. Notably, melasma can arise from two primary causes: i) diffuse-acquired hypermelanosis, and ii) post-inflammatory hyperpigmentation [2, 3].

Cosmetics can be developed using natural compounds rich in biologically active substances, particularly antioxidants. It has been demonstrated that natural resources contain various bioactive compounds. These compounds have garnered significant attention due to their cost-effectiveness, non-toxicity, and substantial benefits [4, 5]. In local preparations derived from the natural metabolites of mushrooms, kojic acid (KJA) and its by-products inhibit tyrosinase activity [6]. Several products containing KJA are used for skin-whitening, antifungal, and antimicrobial purposes [7-9]. Moreover, KJA is a chelator for iron (Fe^{3+}) and copper (Cu^{2+}) metals. Due to its ability to scavenge free radicals, it is used for skin rejuvenation and wrinkle reduction [10]. Despite its potential, KJA faces limitations in absorption due to its hydrophilic nature, which presents challenges in formulation [11]. Issues such as low permeability, inappropriate biodistribution, low hydrolytic degradation, low bioavailability, and a short half-life must be addressed when utilizing this compound. However, combining KJA with molecules such as lipids, proteins, and polymers can help overcome these challenges [12-14]. The enhancement of hydrophilic drug delivery systems can be achieved using polymeric nanoparticles, enabling targeted delivery and transport of the material to its specific location [15].

Many biopolymers and biodegradable polymers have been developed to encapsulate products suitable for cosmetic applications. Among natural nanomaterials, nanoparticles derived from alginates are the most commonly used and deserve special attention. Alginate-based systems are utilized in the cosmetics and healthcare industries to improve stability and protect encapsulated compounds from UV light, temperature fluctuations, and the stomach's acidic environment in the case of oral consumption [16, 17]. Alginate-based nanoparticles are biocompatible, biodegradable, and non-toxic, making them ideal for loading various materials, including anti-melanogenesis agents [18].

The present exploration aimed to develop alginate nanoparticles containing KJA formulations for effective drug delivery to the skin to achieve anti-melanogenesis effects. The potential cutaneous irritation caused by these compounds was also assessed. Additionally, the safety of cells exposed to KJA-containing alginate nanoparticles was evaluated. This study further investigated the effects of these compounds on melanin synthesis and the auto-oxidation of L-DOPA. Based on the results, using KJA-entrapped alginate nanoparticles in cosmetic products for skin applications is recommended as an alternative to traditional methods.

MATERIALS AND METHODS

Materials

Kojic acid (KJA), sodium alginate with a molecular weight of 120,000, calcium chloride ($CaCl_2$), 3-(4,5-dimethylthiazol-2-yl)-2,5-diphenyl-2H-tetrazolium bromide (MTT), dimethyl sulfoxide (DMSO), and L-dopa were purchased from Merck (Darmstadt, Germany). Additionally, Carbopol 934 was obtained from B.F. Goodrich, USA. Distilled water was prepared using a Human Power 2 system (Human Co., Korea) for further purification. All materials were of analytical grade and used without further purification.

Fabrication of KJA-loaded alginate (AL) nanoparticles (KJA-AL-NP)

This study prepared KJA-AL nanoparticles (KJA-AL-NP) using the ionic gelation method. First, sodium alginate (AL) at a concentration of 0.2% (w/v) was added to deionized water, and the solution was stirred at 500 rpm at room temperature (25 °C) for 20 minutes. Meanwhile, a 2.5 mg/mL solution of calcium chloride ($CaCl_2$) was prepared using deionized water. Next, 200 mg of kojic acid (KJA) was added to the AL solution. The KJA-AL nanoparticles were formed by gradually adding varying volumes of the $CaCl_2$ solution to the AL solution (0.2% w/v) while stirring rapidly at 1500 rpm for 30 minutes (see Table 1). The resulting mixture was then sonicated using a probe sonicator (Bandelin, 3100, Germany) at 20% amplitude for 10 minutes.

Table 1. Formulation composition and physical properties (N=3, Mean+SD)

Formulation	KJA (mg)	AL (mg)	CaCl2 (mg/mL)	AL/CaCl2 volume ratio	Particle size (nm)	PDI	Zeta potential (mv)	EE (%)
F1	200	50	2.5	10:2	1691.767± 118.095	0.759±0.008	-29.533±1.331	8.051±3.035
F2	200	50	2.5	10: 4	901.266±3.750	0.666±0.014	-26.233±0.750	23.803±2.426
F3	200	50	2.5	10: 6	607.2±7.748	0.408±0.012	-21.7667±1.569	37.931±3.557
F4	200	50	2.5	10:8	453.2±8.104	0.353±0.012	-19.000±1.569	56.789±3.356
F5	200	50	2.5	10:10	338.533± 8.429	0.296±0.005	-14.566± 0.737	78.770±3.155

Nanoparticle characterization

The mean diameter, polydispersity index (PDI), and zeta potential (ZP) of the corresponding nanoparticles were measured using a ZetaSizer Nano-ZS device and dynamic light scattering (DLS) (Malvern Instruments Ltd., UK). A Cary 630 FTIR spectrophotometer (Agilent Technologies Inc., CA, USA), equipped with a diamond attenuated total reflectance (ATR) accessory, was used to study the interaction between the constituents. The spectra were recorded in the 4000–400 cm^{-1} range with a resolution of 2 cm^{-1}. Differential scanning calorimetry (DSC) analysis was performed using a Pyris-6 DSC instrument (PerkinElmer, Norwalk, USA). Nanoparticles were examined under transmission electron microscopy (TEM) (Philips EM 208S) to assess their morphological characteristics and structural properties.

Producing KJA simple gel and KJA-AL nanoparticle gel

The KJA-AL nanoparticle dispersion (200 mg KJA) in water, containing 0.1% sodium benzoate, was mixed with Carbopol 934 (1% w/v) and kept overnight to ensure uniform distribution. Subsequently, to neutralize the Carbopol in the KJA-AL nanoparticle dispersion, 100 mg of triethanolamine was added and dispersed using a propeller homogenizer at 500 rpm. Finally, a simple KJA gel was prepared by mixing the KJA solution (200 mg KJA) with Carbopol 934 (1% w/v) using the propeller homogenizer at 500 rpm.

Encapsulation Efficacy Evaluation (EE%)

After centrifugation of the KJA-AL nanoparticles at 13,000 rpm for 45 minutes (Sigma 3–30 ks refrigerated centrifuge, Germany), the supernatant was filtered through a 0.22 µm filter. The nanoparticles' encapsulation efficiency (EE%) was determined using Kneuer HPLC (Germany). HPLC analysis used a Hector C18 column (5 µm, 4.6 × 250 mm) with a 0.7 mL/min flow rate. The mobile phase consisted of a mixture of deionized fresh degassed water and acetonitrile in an 80:20 (v/v) ratio, with detection conducted at 268 nm. The area under the curve (AUC) of the filtered supernatant was used to calculate the concentration of the free active ingredient. Encapsulation efficiency was calculated using Equation (1).

$$\boldsymbol{EE}\% = \frac{\boldsymbol{Winitial - Wfree}}{\boldsymbol{Winitial}} \qquad (1)$$

In Vitro drug release

The immersion apparatus was submerged using a cellulose acetate membrane (MWCO of 12 kDa) for *in vitro* pharmaceutical release testing. One gram of the optimized gel formulation was separated in the first step. Before placing the gel into the immersion cell, an assay showed that it contained 5 mg of KJA per gram of gel. The gel was then inserted into the immersion cell. In the next step, specimens containing 5 mg of KJA per gram of gel were placed into the cells. They were sealed with a cap after covering the cells with a cellulose acetate membrane. The cells were then placed into the USP dissolution apparatus II. The rotation speed of the apparatus was set to 100 rpm, and the target temperature was maintained at 37 °C, with 450 mL of dissolution medium (water) added to each vessel. At 0.5, 1, 2, 4, 6, 8, and 24 hours, 5 mL of dissolution medium was filtered through a 0.22 µm filter paper. The active substance in the specimens was measured using an HPLC instrument at a wavelength of 268 nm, following the method described in section 2.5. A calibration curve with a 5–25 µg/mL concentration range and an R^2 value of 0.999 was used to quantify the drug content. After each sample collection, 5 mL of water was added to the dissolution medium to maintain a constant final volume.

Dermal absorption assay

All male Wistar rats in the study weighed approximately 120 to 150 grams. The rats were sedated with 100 µL of ketamine (87 mg/kg) and 25 µL of xylazine (13 mg/kg) before trimming the abdominal skin with an electric razor. Euthanasia was performed by chloroform inhalation after 48 hours, followed by surgical removal of their abdomens. For the skin penetration test, the skin was carefully separated from the underlying subcutaneous fat and immersed in a saline solution for 24 hours at 4°C. Franz diffusion cells with a diffusion area of 3.8 cm^2 were used to place the skin

samples, ensuring that the skin's dermis was in direct contact with the receptor medium. The receiving chamber was filled with deionized water, and the diffusion cells were maintained at 32 ± 0.5°C with stirring at 150 rpm. KJA-AL nanoparticle and KJA simple gel (1 g, 0.5% w/w) were uniformly applied to the donor compartment. It should be noted that KJA simple gel was used as the control sample in this experiment. At 2, 4, 6, 8, 10, and 24 hours, 5 mL of the sample was withdrawn from the receptor phase, ensuring that the removed volume was replaced to maintain a constant total volume. The obtained solution was analyzed by HPLC at 268 nm, following the method outlined in section 2.5, to measure the amount of drug.

Dermal deposition assessment

After completing the skin absorption test, the skins were washed three times with purified water and cleaned. The dermal layer was then dried to measure and calculate the amount of residual KJA. The separated skins were transported in a tube and crushed into small pieces using shears. Next, digestion was performed with deionized water, and the mixture was sonicated for one hour using an ultrasonic bath. Finally, the supernatant was filtered first through Whatman filter paper, followed by a syringe filter with a pore size of 0.22 µm. The obtained solution was analyzed by HPLC at 268 nm, following the method described in section 2.5, to measure the amount of drug.

MTT examination

The present study evaluated cytotoxicity on the HFF (Human Foreskin Fibroblast) cell line and B16F10 cells to gather more information. The cell lines used in this study were obtained from the National Cell Bank (Pasteur Institute of Iran, Tehran, Iran). In the following step, 5×10^3 cells were exposed to various concentrations of KJA-AL nanoparticles, AL nanoparticles without KJA, free KJA, and the carrier control, including 1000, 500, 250, 100, 50, and 25 µM, in the bottom of 96-well microplates and incubated overnight (24 h). After washing the cells with PBS, formazan dye formation was assessed using the MTT assay to evaluate the number of surviving cells. The cells were incubated with a solution containing 0.5 mg/mL of MTT at 37 °C for 4 hours. The supernatant was removed, and the formazan crystals were dissolved in 100 µL of DMSO. After stirring the plates for 20 minutes, the optical density (OD) was measured at a wavelength of 560 nm using a multi-well spectrophotometer. Different concentrations ranging from 31.25 to 1000 µM were tested in this experiment. The experiments were repeated three times, and six control groups (cells in medium) were included. The percentage of surviving cells was calculated using the following formula [19]:

$$Cell\ safety\% = [OD560\ (sample)/OD560(control)] \times 100$$

Melanin content assessment

In this test, melanoma cells (B16F10) were obtained from the Pasteur Institute of Iran. To determine the amount of melanin, 5×10^4 B16F10 cells were seeded in RPMI medium containing 10% (v/v) fetal bovine serum (Gibco, USA) and 1% (v/v) Penicillin/Streptomycin, and placed in a 12-well plate. The cells were then incubated for 24 hours under conditions of 37 °C, 5% CO_2, and 85% humidity. After treatment with different concentrations of KJA aqueous solution and the optimized KJA-AL nanoparticle formulation, the cells were incubated for 24 hours. The cell pellets were digested with 100 µL of 2 M sodium hydroxide (NaOH) and heated at 100 °C for 30 minutes. The amount of melanin in the samples was compared to the control by measuring absorbance at 405 nm using a BioTek spectrophotometer (Winooski, USA).

Anti-L-DOPA auto-oxidation activity

The measurement of L-DOPA auto-oxidation was studied using different concentrations of KJA and KJA-AL nanoparticles, including 1000, 500, 250, 100, 50, and 25 µM. In this assay, 10 mM L-DOPA was mixed with different concentrations of the test samples in 0.1 M sodium phosphate buffer (pH 6.5), with a final volume of 300 µL. Distilled water was used as the negative control. The samples were then incubated at 30 °C for 15 minutes. Changes in light absorbance at a wavelength of 475 nm were measured to evaluate the inhibitory activity.

Animals

In this study, male Wistar rats weighing between 150 and 200 grams were used. Nine rats were housed in each acrylic cage in the animal room, where the temperature was maintained at 21 ± 2 °C, and a 12-hour light-dark cycle was followed. The lights were on from 7:00 AM to 7:00 PM. It is important to note that food was continuously provided to the rats throughout the study, and each rat was evaluated only once.

Cutaneous sensitivity trial

This experiment was conducted by shaving the hair on the dorsal surfaces of the rats using an electric shaver one day before the experiment. The animals were divided into five groups, each consisting of six rats. Groups 2, 3, 4, and 5 were exposed to KJA-AL nanoparticle gel, KJA gel, blank

nanoparticle gel, and a 0.8% (v/v) aqueous solution of formalin (used as the standard sensitizing agent), respectively. Group 1 was designated as the control group. These materials were applied daily for one week. The same researcher regularly evaluated the individual sites using a visual rating system.

Statistic assay

The data obtained in this study are presented as the mean ± standard deviation (SD). Statistical analysis was performed using ANOVA, followed by Tukey's LSD post-hoc test. Data analysis was conducted using SPSS version 22.0 (IBM Co., USA). A t-test was used to compare skin absorption and retention after 24 hours. Statistical significance was considered at $p < 0.05$.

RESULTS AND DISCUSSION

Characterization of KJA-AL-nanoparticle

We successfully synthesized AL nanoparticles loaded with KJA using ionic gelation and ultrasonication. To optimize the production of KJA-AL nanoparticles, different amounts of AL and varying proportions of $CaCl_2$, including 10:2, 10:4, 10:6, 10:8, and 10:10 (v/v), were investigated. The characteristics of the nanoparticles are summarized in Table 1. As shown in Table 1, when the ratio of AL to $CaCl_2$ increased from 10:2 (F1) to 10:10 (F5), the diameter of the nanoparticles significantly decreased from 1691.767 ± 118.095 nm to 338.533 ± 8.429 nm ($P < 0.001$). The formation of nanoparticles is primarily influenced by the interaction of the functional groups of the AL chains, leading to the formation of a complex structure between the carboxylic acid groups and calcium ions. Previous studies have indicated that a higher amount of AL results in more functional groups being available to interact with calcium, promoting the formation of a larger number of complexes with calcium cations. These findings are consistent with those of previous studies [20], which suggests that increasing the amount of AL in the formulation leads to larger particle sizes. Conversely, higher calcium ion content reduces the number of polymer chains, resulting in smaller nanoparticles. Therefore, it can be concluded that increasing the amount of calcium chloride leads to a smaller particle size [21].

The PDI results ranged between zero and one. The closer the values are to zero, the more homogeneous the dispersion [22]. Table 1 shows PDI values ranging from 0.296 ± 0.005 to 0.759 ± 0.008 ($P < 0.01$). These results suggest that monodispersity increases as the AL/$CaCl_2$ ratio is increased. Previous studies have also emphasized that increasing the amount of calcium chloride produces smaller dispersions [21].

The encapsulation efficiency (EE%) of the samples is reported in Table 1. The EE% of the KJA-AL nanoparticle preparations ranged from 8.051 ± 3.035% to 78.770 ± 3.155%. The data clearly show that as the mass ratio of calcium chloride increased (from 10:1 to 10:10), the EE% also increased. This can be attributed to forming intermolecular and intramolecular bonds under the influence of calcium cations. The interaction between the negatively charged carboxylic acid groups and calcium cations enhances gelation in the aqueous phase. In this study, nanoparticles were formed immediately after mixing the $CaCl_2$ and AL solutions; however, the AL/$CaCl_2$ ratio significantly affected the EE%. The formation of hydrogen and electrostatic bonds between AL, calcium ions, and drug molecules during nanoparticle production increases the EE%. On the other hand, decreasing the AL/$CaCl_2$ ratio increases viscosity, which may explain the reduced entrapment efficiency and an increase in nanoparticle size. The results suggest that the optimum amount of calcium chloride leads to the production of nanoparticles. When a high volume of calcium chloride is used, divalent calcium creates microdomains with high alginate concentrations. This phenomenon is likely due to an imbalance between the calcium ions and the alginate binding sites as the amount of calcium per unit volume increases. As a result, calcium cations form cross-links between glucuronic acid residues, creating network gel aggregates and increasing drug encapsulation [23]. Previous research has shown that using small amounts of calcium chloride resulted in more binding sites on alginate than available calcium ions, preventing the formation of well-organized nanoparticles with appropriate density and encapsulation capacity [24].

As shown in Table 1, a reduction in the zeta potential of the nanoparticles was observed with an increase in the AL/$CaCl_2$ ratio. The zeta potential for the AL/$CaCl_2$ ratio of 10:2 was -29.533 ± 1.331 mV, whereas at a ratio of 10:10, the zeta potential decreased to -14.566 ± 0.737 mV (less negative). Previous studies have indicated that the zeta potential increases as the KJA encapsulation ratio decreases. This could be due to factors such as: i) the distribution of free KJA and AL in the aqueous phase or the potential diffusion layer, and ii) the formation of hydrogen and electrostatic interactions between Ca^{2+} and drug molecules during the production of AL nanoparticles [15, 25].

In the present study, the optimal nanoparticles exhibited characteristics such as a small particle diameter, narrow PDI, and a high EE% value. The

production of nanoparticles with these characteristics demonstrates the study's high accuracy. Among the formulations, F5 was selected for further investigations, as it had the smallest diameter (338.533 ± 8.429 nm), the highest encapsulation efficiency (78.770 ± 3.155%), and a PDI value of 0.296 ± 0.005.

TEM examination

In the present study, the best formulation was F5, which was selected for microscopic analysis (Fig. 1). Figure 1 shows that all the nanoparticles observed in the image have uniform sizes and distinct spherical shapes.

DSC results

The DSC thermogram analysis for KJA, sodium alginate, and lyophilized optimized KJA-AL nanoparticles is shown in Figure 2. The endothermic peak observed at 153.56°C in the DSC thermogram corresponds to KJA. For sodium alginate, the DSC thermogram shows an endothermic peak at 90.49°C and an exothermic peak at 248.42°C. The endothermic peak related to sodium alginate is likely due to the loss of water and moisture from the polysaccharide, while the exothermic peak can be attributed to the thermal decomposition of the material [26]. A comparison of the DSC peaks in Figure 2 shows that the melting peak of the drug is absent in the F5 formulation. This observation suggests that, during the preparation process, KJA dissolves into the polymer matrix, resulting in the drug being in an amorphous phase.

ATR-FTIR results

ATR-FTIR analysis was performed to investigate the potential chemical interactions between the drug and other nanoparticle components in the structure of AL nanoparticles. The ATR-FTIR spectra of KJA, AL, and the KJA-AL nanoparticle (F5) are shown in Figure 3 and Table 2. The results from the ATR-FTIR analysis indicated that there were no chemical interactions between KJA and the other components in the nanoparticle.

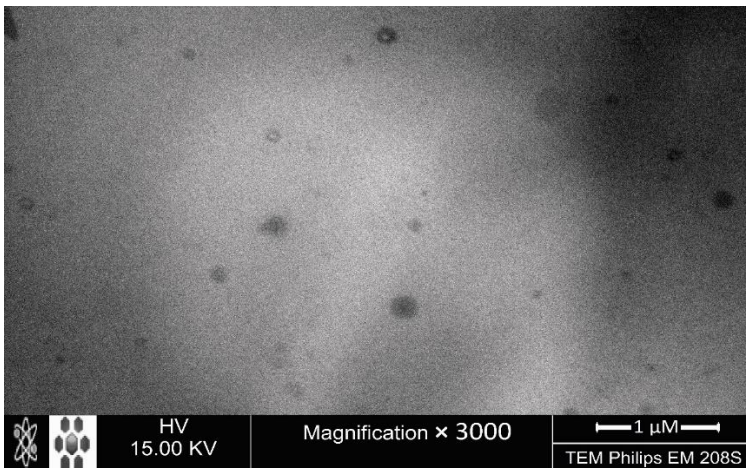

Fig. 1. TEM image of optimum formulation KJA-AL-nanoparticle (F5)

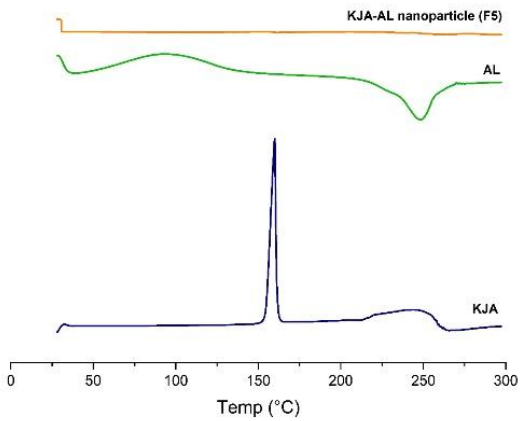

Fig. 2. DSC thermo-gram of KJA- AL nanoparticle (F5), AL and KJA

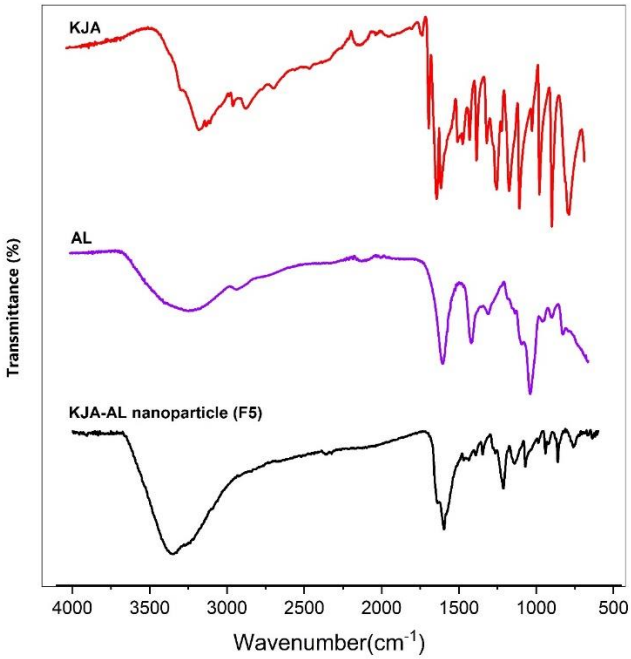

Fig. 3. ATR-FTIR spectra for KJA, AL and KJA-AL nanoparticle (F5)

Table 2. Wavenumber and functional groups of main substance of NP

Material	Wavenumber (cm^{-1})	Functional groups
KJA	3253, 3143	O-H stretching vibrations
	2923, 2841	aliphatic C-H stretching
	1656	C=O stretching of ring
	1605	C=C stretching
	1071	C-O stretching
AL	3236	O-H stretching
	2926	C-H stretching
	1591, 1406	asymmetric and symmetrical stretching of carboxylate
	1080, 1025	C-O stretching

KJA release assay

One of the factors influencing nanoparticle drug release is drug bioavailability. The present study investigated drug release from the F5 gel and KJA simple gel, and their release behaviors are shown in Figure 4. The results indicated that the release rate of KJA from the F5 gel was 50.976 ± 1.579% in the first two hours, and after 24 hours, the release reached 67.840 ± 2.428%. In contrast, the release data showed that the KJA nanoparticles were released at a controlled rate, with the drug release from the nanoparticle matrix to the medium occurring at a uniform speed. The KJA solution, however, released the drug immediately, with approximately 95% of the drug being released in the first two hours.

Previous studies have shown that AL nanoparticles of timolol maleate exhibit stable and uniform release over 24 hours [21]. Polymer nanoparticles also demonstrate uniform and regulated release, influenced by several factors: i) Surface pores are typically exposed to diffusion due to concentration gradients, ii) Salts present in the buffers facilitate screening interactions between the drug and the vehicle, and iii) Electrostatic interactions are reduced when carboxylate groups are protonated. Swelling and charge screening also affect drug release from the vehicles and the transfer of the drug from particles to surfaces. Modifying these parameters can shift the release profile from a fast release stage to an extended release. Conversely, strong electrostatic interactions between the drug and vehicle can enhance drug encapsulation, decreasing the release rate [27].

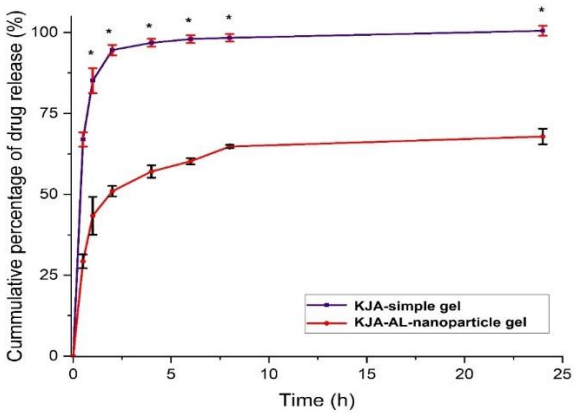

Fig. 4. Release profile of KJA-simple gel and KJA-AL-nanoparticle (F5). KJA-AL-nanoparticle (F5) release less KJA than KJA-simple gel during 24 h significantly ($p<0.05$) (n=3) *($p<0.05$).

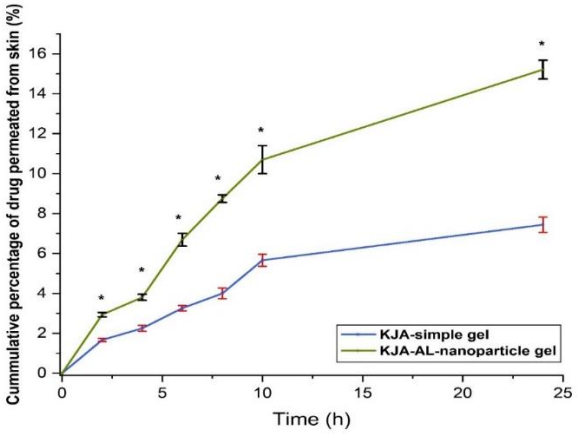

Fig. 5. Collective extent of KJA simple gel and KJA-AL- nanoparticle gel (F5) penetrated through rat skin. *($p<0.05$)(n=3).

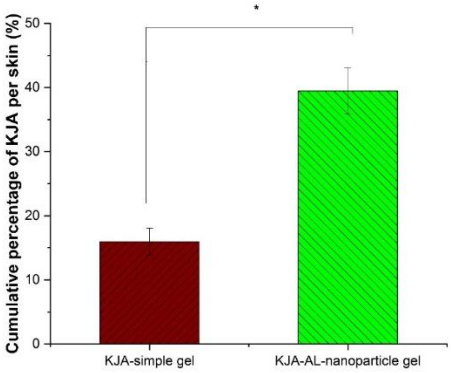

Fig. 6. Collective extent of KJA depot in skin from KJA simple gel and KJA-AL-nanoparticle gel (F5). *($p<0.05$) (n=3).

EX-vivo transdermal and dermal trial

Figure 5 shows the transdermal delivery (accumulation of KJA penetrated through rat skin) for KJA-AL nanoparticle gel (F5 gel) and KJA simple gel, while dermal delivery (level of KJA permeated to the skin layers) is presented in Figure 6. A comparison between the KJA-AL nanoparticle gel (F5 gel) and KJA simple gel shows that the F5 gel exhibits greater penetration into the dermal layers, making it more suitable for transdermal delivery ($p < 0.05$). In the receptor compartment, the highest level of KJA was detected for the KJA simple gel (7.437 ± 0.384% or 97.878 ± 8.752 µg/cm²), while higher values (15.210 ± 0.468% or 200.170 ± 6.161 µg/cm²) were obtained for the KJA-AL nanoparticle gel (F5 gel) ($p < 0.05$). A comparison of the KJA-AL nanoparticle gel (F5 gel) and the KJA simple gel revealed that the remaining KJA content was 39.470 ± 3.606% or 519.432 ± 47.465 µg/cm² for F5 gel, compared to 5.968 ± 2.107% or 210.150 ±

21.669 µg/cm² for KJA simple gel ($p < 0.05$). This value was significantly higher for the F5 gel than for the KJA simple gel. The results of this study indicate that the use of AL nanoparticles, compared to traditional gels, is more effective for local targeting.

Many skin care products contain AL nanoparticles due to their potential benefits for the skin [16]. Various factors influence the absorption of AL nanoparticles into the skin, as the skin is a complex structure with multiple layers and functions. Smaller AL nanoparticles tend to penetrate the skin more readily than larger ones, resulting in a higher absorption rate for the smaller nanoparticles. The size of natural polymer and biopolymer nanoparticles typically ranges from 20 to 700 nm (338 nm in this study), and the small size of the nanoparticles enhances their ability to penetrate the outer layer of the skin [16, 28].

Surface charge plays a significant role among the factors that affect the skin penetration of nanoparticles, though its impact warrants further investigation. Previous research has shown that the diffusion of negatively charged nanoparticles is slower in the skin matrix, as they form electrostatic interactions with the stratum corneum [29].

On the other hand, hair follicles are one of the primary routes for the absorption of AL nanoparticles into the skin, as they contain small pores that typically facilitate the penetration of topical products. AL nanoparticles, being small in size, can penetrate deeper layers of the skin through the pores of the hair follicles [30].

In general, the absorption process of polymeric nanoparticles is complex and influenced by several factors, necessitating further investigation. However, extensive research is being conducted to evaluate the potential of nanoparticles to enhance skin health and appearance. These studies may provide valuable insights into the mechanisms of action of these nanoparticles.

Previous studies have shown that KJA-hydrogel containing AL exhibits higher skin penetration than typical semisolid formulations. Additionally, formulations containing AL have demonstrated promising effects for treating hyperpigmentation disorders [18].

Cytotoxicity test

The potential cytotoxic effects of different concentrations (from 25 to 1000 µM) of KJA, F5, and blank nanoparticles were studied on HFF (normal fibroblast) and B16F10 cell lines. Studies on the effects of F5 and KJA on normal cells (HFF fibroblast cells) showed a significant decrease in cell survival after 24 hours (Fig. 7a). A comparison between F5 and KJA revealed that the percentage of surviving HFF cells after exposure to these formulations was higher for F5 (84% vs. 78%) (Fig. 7a). Conversely, the survival rate of B16F10 melanoma cancer cells decreased significantly over 24 hours after exposure to both formulations ($p < 0.05$) (Fig. 7b). A comparison of the effects of KJA and F5 on the B16F10 cell line (after 24 hours) showed that the percentage of cell death was lower for KJA than for F5 (51% vs. 40%) ($p < 0.001$) (Fig. 7b).

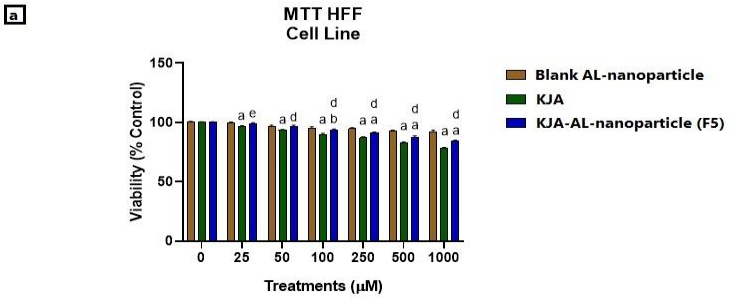

[a] p<0.001 compared with Nano-Blank, [b] p<0.01 compared with Nano-Blank, [d] p<0.001 compared with Kojic Acid, [e] p<0.01 compared with Kojic Acid

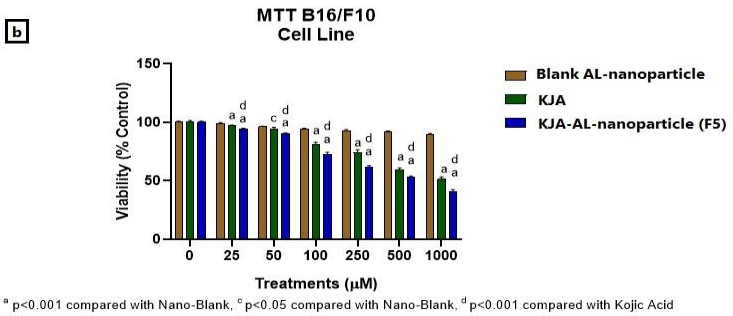

[a] p<0.001 compared with Nano-Blank, [c] p<0.05 compared with Nano-Blank, [d] p<0.001 compared with Kojic Acid

Fig. 7a. The percentage of surviving HFF cells at varied concentrations of KJA, blank AL-nanoparticle and KJA-AL-nanoparticle (F5) (data are mean± SD) (n=6). Fig. 7b. The percentage of surviving B16F10 cells at varied concentrations of KJA, blank AL-nanoparticle and KJA-AL-nanoparticle (F5) (data are mean± SD) (n=6).

The medicinal toxicity of nanoparticles on various body organs is well-documented, and studies have shown that smaller nanoparticles can more readily enter cells, potentially causing more significant toxicity. The interaction between cells, proteins, and nanoparticles can be enhanced by their surface charges. The electrical charge imparted by nanoparticles can also induce toxic effects on other organs [31].

Prevention of L-DOPA auto-oxidation examination

Skin melanogenesis plays a crucial role in beauty and significantly affects the quality of life for patients, making anti-melanogenic products essential [32]. This study suggests a concentration-dependent mechanism by which free KJA and the F5 formulation inhibit the spontaneous oxidation of L-dopa. As shown in Figure 8, the inhibition level for KJA solution at a concentration of 1000 µM was 55.829 ± 2.881%. An increase in inhibition is observed with the F5 formulation, which reached 82.224 ± 2.079% at the same concentration. There are several mechanisms by which KJA colloidal nanoparticles prevent the auto-oxidation of L-dopa. The KJA compound can chelate iron and copper ions during the oxidation process. When these ions bind to KJA, the catalysis of L-dopa oxidation is inhibited [33]. Additionally, KJA acts as an antioxidant, preventing auto-oxidation by neutralizing free radicals. This reduces the involvement of free radicals in the oxidative damage of L-dopa [18, 34]. The results indicate that combining KJA with AL nanoparticles effectively inhibits auto-oxidation, making it a promising ingredient for skin lightening in cosmetic products.

Melanin content investigation

This test measured the amount of intracellular melanin in the B16F10 cell line. The results indicate that, unlike the blank solution, which significantly affected melanin content, the free KJA solution and the F5 formulation inhibited melanin synthesis. The evaluation of melanogenesis shown in Figure 9 reveals that, after treatment with different concentrations of KJA and F5 (including 1000, 500, 250, 100, 50, and 25 µM), a decrease in melanin content was observed. The highest inhibition percentages were 54.379 ± 0.964% for KJA and 41.971 ± 1.743% for F5 at 1000 µM (Figure 9).

The melanin depot was reduced by the F5 compound during typical melanin synthesis, with its inhibitory effect being significantly greater than that of the free KJA solution and blank nanoparticles. Previous studies have shown that KJA is a direct tyrosinase inhibitor and prevents its activity [35-37]. Tyrosinase plays a critical role in the key steps of melanogenesis, and since it is a rate-limiting enzyme, its inhibition results in a significant decrease in melanin production [38]. Therefore, it can be concluded that compounds that inhibit tyrosinase activity or reduce its expression may be promising candidates for further research to develop new anti-pigmentation drugs. Additionally, loading KJA into nanoformulations can enhance its absorption rate, contributing to greater efficacy.

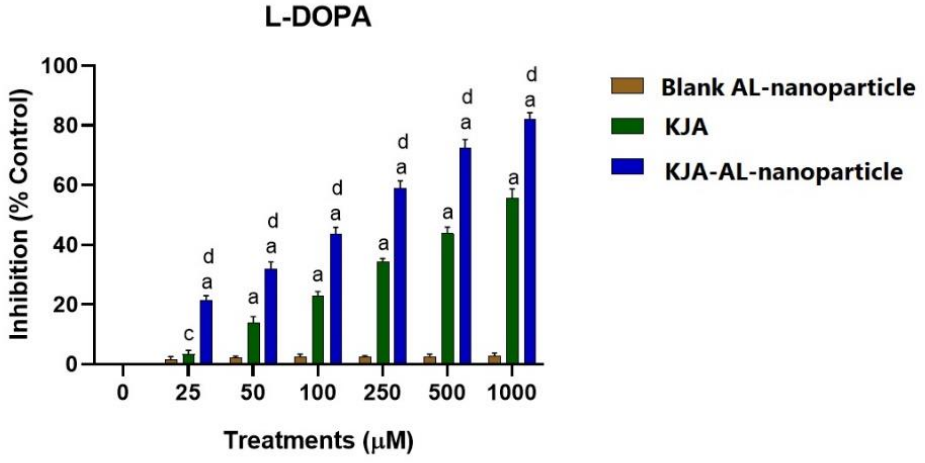

[a] p<0.001 compared with Nano-Blank, [c] p<0.05 compared with Nano-Blank, [d] p<0.001 compared with Kojic Acid

Fig. 8. L-Dopa auto-oxidation prevention action of KJA, Blank AL-nanoparticle, and KJA-AL-nanoparticle (F5) (mean±SD) (n=6).

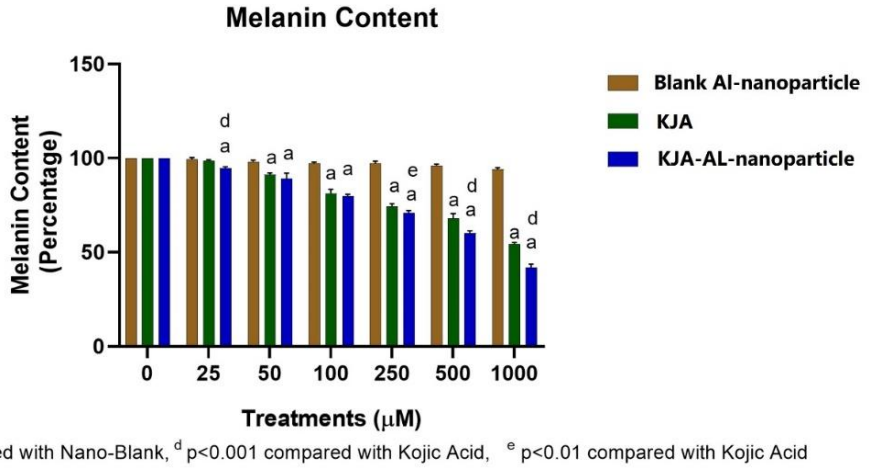

Fig. 9. Percent of melanin content of KJA, plain blank AL-nanoparticle and KJA-AL- nanoparticle (F5) (mean±SD) (n=6).

Animal sensitivity trails

Any nanoparticle used for drug delivery not only releases the medication but can also have significant side effects. When using KJA nanoparticle gel in cosmetics, it is essential to minimize cutaneous sensitivity reactions to the lowest possible level, ensuring the product remains harmless [39]. Skin sensitivity is a critical side effect for dermal products, and the extent of this complication is directly related to the drug dosage. Reducing side effects can be achieved by modulating drug release, enhancing absorption into the follicle, and limiting cutaneous diffusion [40].

The data in Table 3 and Figure 10 show the effect of different products on skin sensitivity, including swelling and redness. According to the Woodward, Draize, and Calvery scale, non-irritating skin materials have a rating of 2 or less. In this study, the F5 gel formulation did not cause itching, was well-tolerated by the patient, and improved the skin condition. It can be concluded that the F5 gel is effective for dermatological use on human skin and can safely reduce hyperpigmentation symptoms.

Table 3. Skin irritation scores following topically administration

	Control		**KJA-AL-nanoparticle gel (F5)**		**KJA-simple gel**		**blank AL-nanoparticle gel**		**Formalin**	
Rat num	[a]Erythema	[b]Edema	Erythema	Edema	Erythema	Edema	Erythema	Edema	Erythema	Edema
1	0	0	0	0	0	0	0	1	4	3
2	0	0	0	0	0	0	1	0	3	4
3	0	0	0	0	0	0	0	1	3	3
4	0	0	0	0	1	1	0	0	4	3
5	0	0	0	1	1	0	0	0	3	3
6	0	0	1	0	0	1	1	0	4	4

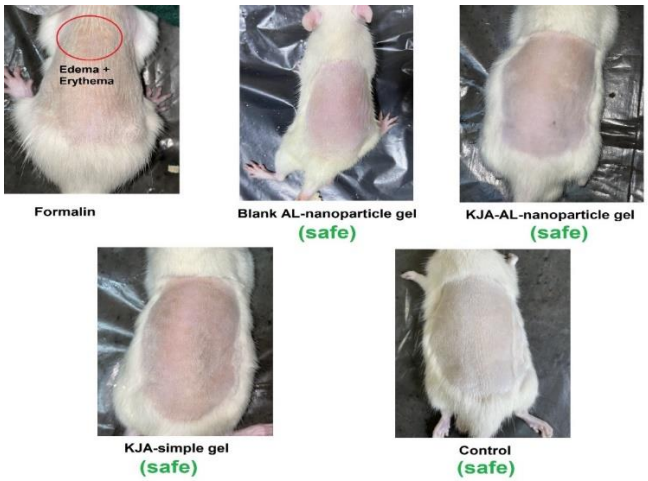

Fig. 10. Skin sensitivity results of various preparation.

Sodium alginate is a safe, semi-synthetic substance commonly used in cosmetics, particularly in skin care products, due to its high biocompatibility with the skin. This non-toxic substance moisturizes the skin and protects it without blocking pores. It is approved for use in cosmetics by regulatory agencies [41].

Studies on the skin irritation potential of KJA and menadione-loaded biopolymer hydrogel containing AL demonstrated that this formulation does not cause skin irritation [18, 42].

CONCLUSION

KJA (a hydrophilic substance) was effectively incorporated to produce AL nanoparticles from a natural polymer. A solid-state test demonstrated that KJA in the AL nanoparticles existed in an amorphous form without chemical interaction. In this study, various parameters related to the KJA-loaded AL nanoparticle topical preparation were obtained, including average EE%, PDI, particle size, and zeta potential: 78.770 ± 3.155%, 338.533 ± 8.429 nm, 0.296 ± 0.005, and -14.566 ± 0.737 mV, respectively. Based on the skin permeation test results, the KJA-AL nanoparticle gel penetrated skin layers and receptor chambers more effectively than the KJA simple gel. The MTT test on human foreskin fibroblasts (HFF) revealed lower cytotoxicity, with nearly 84% of the cells surviving after exposure to the KJA-loaded AL nanoparticles. AL nanoparticles loaded with optimal amounts of KJA exhibited more cytotoxicity than the KJA solution against melanoma cancer cells (B16F10). Furthermore, a dermal irritation test showed no irritation caused by the KJA-AL nanoparticle gel constituents. A comparison of pure KJA and blank AL nanoparticles showed that the anti-hyperpigmentation activity, reduction in melanin development, and inhibition of L-Dopa auto-oxidation were more pronounced in the AL nanoparticles loaded with KJA. The findings of this research demonstrate that AL nanoparticles entrapped with KJA have significant potential for use in pharmaceuticals and cosmetics as anti-hyperpigmentation agents. AL nanoparticles loaded with KJA, as natural nanoparticles, can help modernize the cosmeceutical market due to: i) specific drug delivery, ii) enhanced bioavailability, and iii) improved therapeutic efficacy. However, thorough evaluation of their safety and efficacy in cosmeceutical applications and optimization of manufacturing processes will be necessary to ensure cost-effectiveness and scalability.

ACKNOWLEDGMENT

The authors would like to express their sincere and special appreciation to the research council of Hormozgan University of Medical Sciences, Bandar Abbas, Iran, for their valuable and technical cooperation. Also, this study was funded by a grant number [4020043] from the Hormozgan University of Medical Sciences, Bandar Abbas, Iran. The authors reported no potential conflict of interest.

DISCLOSURE STATEMENT

The authors reported no potential conflict of interest.

FUNDING

This study was funded by a grant number [4020043] from the Hormozgan University of Medical Sciences, Bandar Abbas, Iran.

ETHICAL APPROVAL

As part of the present study, all animal experiments were approved by the ethical committee for Animal Investigation at HUMS with code of= IR.HUMS.REC.1402.073. All animal experiments followed ARRIVE protocols (Animal Research: Reporting of *in vivo* Experiments) and were under instructions of the UK Animals (Scientific Procedures) Act 1986 and EU Directive 2010/63/EU on animal experimentation.

DATA AVAILABILITY STATEMENT

All datasets generated for this study are included in the article.

REFERENCES

1. Levy LL, Emer JJ. Emotional benefit of cosmetic camouflage in the treatment of facial skin conditions: personal experience and review. Clin Cosmet Investig Dermatol. 2012:173-182.
2. García CG. Lesiones de la pigmentación cutánea. Medicine: Programa de Formación Médica Continuada Acreditado. 2010;10(48):3195-3203.
3. Mohammadian E, Foroumadi A, Hasanvand Z, Rahimpour E, Zhao H, Jouyban A. Simulation of mesalazine solubility in the binary solvents at various temperatures. J Mol Liq. 2022;357:119160.
4. Carvalho IT, Estevinho BN, Santos L. Application of microencapsulated essential oils in cosmetic and personal healthcare products–a review. Int J Cosmet Sci. 2016;38(2):109-119.
5. Barroso MR, Barros L, Dueñas M, Carvalho AM, Santos-Buelga C, Fernandes IP, et al. Exploring the antioxidant potential of Helichrysum stoechas (L.) Moench phenolic compounds for cosmetic applications: Chemical characterization, microencapsulation and incorporation into a moisturizer. Ind Crops Prod. 2014;53:330-336.

6. Abd El-Aziz BA. Improvement of kojic acid production by a mutant strain of Aspergillus flavus. J Nat Sci Res. 2013;3(4):31-41.
7. Liu X, Xia W, Jiang Q, Xu Y, Yu P. Synthesis, characterization, and antimicrobial activity of kojic acid grafted chitosan oligosaccharide. J Agric Food Chem. 2014;62(1):297-303.
8. Kim JH, Chan KL. Augmenting the antifungal activity of an oxidizing agent with kojic acid: Control of Penicillium strains infecting crops. Molecules. 2014;19(11):18448-18464.
9. Bashir F, Sultana K, Khalid M, Rabia H. Kojic acid: a comprehensive review. AJAHS. 2021.
10. Lajis AFB, Hamid M, Ariff AB. Depigmenting effect of kojic acid esters in hyperpigmented B16F1 melanoma cells. Biomed Res Int. 2012;2012.
11. Ookubo N, Michiue H, Kitamatsu M, Kamamura M, Nishiki T-i, Ohmori I, et al. The transdermal inhibition of melanogenesis by a cell-membrane-permeable peptide delivery system based on poly-arginine. Biomaterials. 2014;35(15):4508-4516.
12. Khezri K, Saeedi M, Morteza-Semnani K, Akbari J, Hedayatizadeh-Omran A. A promising and effective platform for delivering hydrophilic depigmenting agents in the treatment of cutaneous hyperpigmentation: Kojic acid nanostructured lipid carrier. Artif Cells Nanomed Biotechnol. 2021;49(1):38-47.
13. Faig JJ, Moretti A, Joseph LB, Zhang Y, Nova MJ, Smith K, et al. Biodegradable kojic acid-based polymers: controlled delivery of bioactives for melanogenesis inhibition. Biomacromolecules. 2017;18(2):363-373.
14. Nawarak J, Huang-Liu R, Kao S-H, Liao H-H, Sinchaikul S, Chen S-T, et al. Proteomics analysis of kojic acid treated A375 human malignant melanoma cells. J Proteome Res. 2008;7(9):3737-3746.
15. Saeedi M, Morteza-Semnani K, Siahposht-Khachaki A, Akbari J, Valizadeh M, Sanaee A, et al. Passive Targeted Drug Delivery of Venlafaxine HCl to the Brain by Modified Chitosan Nanoparticles: Characterization, Cellular Safety Assessment, and In Vivo Evaluation. J Pharm Innov. 2023:1-13.
16. Łętocha A, Miastkowska M, Sikora E. Preparation and characteristics of alginate microparticles for food, pharmaceutical and cosmetic applications. Polymers. 2022;14(18):3834.
17. Mohammadian E, Rahimpour E, Alizadeh-Sani M, Foroumadi A, Jouyban A. An overview on terbium sensitized based-optical sensors/nanosensors for determination of pharmaceuticals. Appl Spectrosc Rev. 2022;57(1):39-76.
18. Gatabi ZR, Saeedi M, Morteza-Semnani K, Rahimnia SM, Yazdian-Robati R, Hashemi SMH. Green preparation, characterization, evaluation of anti-melanogenesis effect and in vitro/in vivo safety profile of kojic acid hydrogel as skin lightener formulation. J Biomater Sci Polym. 2022;33(17):2270-2291.
19. Auer SK, Fossati S, Morozov Y, Mor DC, Jonas U, Dostalek J. Rapid Actuation of Thermo-Responsive Polymer Networks: Investigation of the Transition Kinetics. J Phys Chem B. 2022;126(16):3170-3179.
20. Daemi H, Barikani M. Synthesis and characterization of calcium alginate nanoparticles, sodium homopolymannuronate salt and its calcium nanoparticles. Sci Iran. 2012;19(6):2023-2028.
21. Ahdyani R, Novitasari L, Martien R, Danarti R. Formulation and characterization of timolol maleate-loaded nanoparticles gel by ionic gelation method using chitosan and sodium alginate. Int J Appl Pharm. 2019;11:48-54.
22. Taymouri S, Varshosaz J. Effect of different types of surfactants on the physical properties and stability of carvedilol nano-niosomes. Adv Biomed Res. 2016;5.
23. Sarei F, Dounighi NM, Zolfagharian H, Khaki P, Bidhendi SM. Alginate nanoparticles as a promising adjuvant and vaccine delivery system. Indian J Pharm Sci. 2013;75(4):442.
24. Ferreiro MG, Tillman L, Hardee G, Bodmeier R. Characterization of alginate/poly-L-lysine particles as antisense oligonucleotide carriers. Int J Pharm. 2002;239(1-2):47-59.
25. Chen D, Parayath N, Ganesh S, Wang W, Amiji M. The role of apolipoprotein-and vitronectin-enriched protein corona on lipid nanoparticles for in vivo targeted delivery and transfection of oligonucleotides in murine tumor models. Nanoscale. 2019;11(40):18806-18824.
26. Rao KM, Mallikarjuna B, Krishna Rao K, Sudhakar K, Rao KC, Subha M. Synthesis and characterization of pH sensitive poly (hydroxy ethyl methacrylate-co-acrylamidoglycolic acid) based hydrogels for controlled release studies of 5-fluorouracil. Int J Polym Mater Polym Biomater. 2013;62(11):565-571.
27. Harrigan P, Wong K, Redelmeier T, Wheeler J, Cullis P. Accumulation of doxorubicin and other lipophilic amines into large unilamellar vesicles in response to transmembrane pH gradients. Biochim Biophys Acta, Biomembr. 1993;1149(2):329-338.
28. Sharkawy A, Barreiro MF, Rodrigues AE. New Pickering emulsions stabilized with chitosan/collagen peptides nanoparticles: Synthesis, characterization and tracking of the nanoparticles after skin application. Colloids Surf A: Physicochem Eng Asp. 2021;616:126327.
29. Filon FL, Mauro M, Adami G, Bovenzi M, Crosera M. Nanoparticles skin absorption: New aspects for a safety profile evaluation. Regul Toxicol Pharmacol. 2015;72(2):310-322.
30. Główka E, Wosicka-Frąckowiak H, Hyla K, Stefanowska J, Jastrzębska K, Klapiszewski Ł, et al. Polymeric nanoparticles-embedded organogel for roxithromycin delivery to hair follicles. Eur J Pharm. 2014;88(1):75-84.
31. Hashemi SMH, Enayatifard R, Akbari J, Saeedi M, Seyedabadi M, Morteza-Semnani K, et al. Venlafaxine HCl encapsulated in niosome: green and eco-friendly formulation for the management of pain. AAPS PharmSciTech. 2022;23(5):149.
32. Rigopoulos D, Gregoriou S, Katsambas A. Hyperpigmentation and melasma. J Cosmet Dermatol. 2007;6(3):195-202.
33. Khezri K, Saeedi M, Morteza-Semnani K, Akbari J, Rostamkalaei SS. An emerging technology in lipid

research for targeting hydrophilic drugs to the skin in the treatment of hyperpigmentation disorders: kojic acid-solid lipid nanoparticles. Artif Cells Nanomed Biotechnol 2020;48(1):841-853.
34. Saeedi M, Morteza-Semnani K, Akbari J, Rahimnia SM, Ahmadi F, Choubdari H, et al. Development of kojic acid loaded collagen-chitosan nanoparticle as skin lightener product: in vitro and in vivo assessment. J Biomater Sci Polym Ed. 2024;35(1):63-84.
35. Oh M-J, Abdul Hamid M, Ngadiran S, Seo Y-K, Sarmidi MR, Park CS. Ficus deltoidea (Mas cotek) extract exerted anti-melanogenic activity by preventing tyrosinase activity in vitro and by suppressing tyrosinase gene expression in B16F1 melanoma cells. Arch Dermatol Res. 2011;303:161-170.
36. Panzella L, Napolitano A. Natural and bioinspired phenolic compounds as tyrosinase inhibitors for the treatment of skin hyperpigmentation: Recent advances. Cosmetics. 2019;6(4):57.
37. Yu F, Tang X, Qu B, Zhong Z, Zhang W, Yu X. Kojic acid inhibited melanin synthesis by tyrosinase pathway in Pteria penguin. Aquac Res. 2020;51(4):1584-1591.
38. Chang T-S. Natural melanogenesis inhibitors acting through the down-regulation of tyrosinase activity. J Mater. 2012;5(9):1661-1685.
39. Mahant S, Kumar S, Nanda S, Rao R. Microsponges for dermatological applications: perspectives and challenges. Asian J Pharm Sci. 2020;15(3):273-291.
40. Fulton Jr JE, Farzad-Bakshandeh A, Bradley S. Studies on the mechanism of action of topical benzoyl peroxide and vitamin A acid in acne vulgaris. J Cutan Pathol. 1974;1(5):191-200.
41. Additives EPo, Feed PoSuiA, Bampidis V, Azimonti G, Bastos MdL, Christensen H, et al. Safety and efficacy of a feed additive consisting of sodium alginate for all animal species (ALGAIA). EFSA Journal. 2022;20(3):e07164.
42. Rezanejad Gatabi Z, Rahimnia SM, Morteza-Semnani K, Yazdian-Robati R, Hashemi SMH, Saeedi M. Vitamin K (Menadione)-incorporated chitosan/alginate hydrogel as a novel product for periorbital hyperpigmentation. J Biomater Sci Polym Ed. 2024:1-22.